Journal of Chromatography, 499 (1990) 103–124
Elsevier Science Publishers B.V., Amsterdam — Printed in The Netherlands

CHROMSYMP. 1646

HIGH-PERFORMANCE LIQUID CHROMATOGRAPHY OF AMINO ACIDS, PEPTIDES AND PROTEINS

XCV[a]. THERMODYNAMIC AND KINETIC INVESTIGATIONS ON RIGID AND SOFT AFFINITY GELS WITH VARYING PARTICLE AND PORE SIZES: COMPARISON OF THERMODYNAMIC PARAMETERS AND THE ADSORPTION BEHAVIOUR OF PROTEINS EVALUATED FROM BATH AND FRONTAL ANALYSIS EXPERIMENTS[b]

F. B. ANSPACH, A. JOHNSTON, H.-J. WIRTH, K. K. UNGER[c] and M. T. W. HEARN*
Department of Biochemistry and Centre of Bioprocess Technology, Monash University, Clayton, Victoria 3168 (Australia)

SUMMARY

The thermodynamic constants, associated with the interaction of three proteins with triazine dye affinity sorbents, have been derived from bath and frontal analysis experiments. In cases where mass-transfer restrictions are very high, calculation of the thermodynamic constants directly from frontal analysis experiments could not be achieved. In such cases, a portion of the adsorbate was always present in the effluent, a situation which has its effect as the split peak phenomenon. With Fractogel-based triazine dye affinity sorbents none of the test proteins applied in frontal analysis were adsorbed. A similar behaviour was observed for a Cellufine sorbent during the adsorption of human serum albumin and the Blue Sepharose CL6B sorbent during the adsorption of alcohol dehydrogenase, which displayed much slower apparent adsorption kinetics than observed in the bath experiments. These phenomena were shown to be associated with changes in the gel structure, caused in part by the column packing procedure.

Silica-based sorbents performed better in the adsorption of lysozyme in the column mode than soft-gel affinity sorbents, as was evident in the higher capacities and steeper breakthrough curves. At high protein concentrations (feedstock concentration >0.2 mg/ml) breakthrough curves obtained with small- and large-particle-size sorbents, but of constant pore size, were found to be identical. This finding demonstrates that the use of small-particle-size sorbents (*e.g.* particle diameter,

[a] For Part XCIV, see ref. 1.

[b] The authors wish to acknowledge the enormous enthusiasm, insight and scholarship which Csaba Horváth has brought to the field of chromatographic sciences. His example has stimulated them in numerous ways over the past decade to examine in greater detail more systematic methods to elucidate chromatographic processes and phenomena. For these reasons alone, this manucript is dedicated to Csaba Horváth in celebration of his sixtieth birthday.

[c] On sabbatical leave from the Institut für Anorganische Chemie und Analytische Chemie, Johannes Gutenberg-Universität, 6500 Mainz, F.R.G.

0021-9673/90/$03.50

$d_p \leqslant 5$ μm) for the preparative isolation of proteins may not be justified when operating in the overload mode.

With other higher-molecular-weight proteins and the silica-based sorbent systems examined, the small-particle-size sorbents ($d_p = 5$ μm) displayed less symmetrical shapes of their breakthrough curves than the larger-particle-size and soft-gel sorbents. This behaviour was further exacerbated when non-porous glass or silica-based sorbents were utilized. These non-porous affinity sorbents displayed nearly rectangular breakthrough shapes at the onset of the adsorption process, but comparatively slow adsorption kinetics became evident as saturation was approached. This phenomenon has been attributed to surface rearrangement and/or reorientation of the adsorbed proteins, particularly with sorbents of high ligand densities.

INTRODUCTION

The evaluation of thermodynamic data from continuously stirred bath experiments has been addressed in an associated publication[2], including the description of a simple method for comparing apparent adsorption kinetics with different types of affinity sorbents. Such data have been found useful for the prediction of the capacity of affinity sorbents for the preparative chromatographic isolation of proteins. Furthermore, the observed adsorption kinetics in the bath experiments can be related to the breakthrough behaviour of sorbents. Collectively, guidelines, derived from bath experiments, provide a basis for the choice of sorbent for a particular chromatographic isolation procedure. For example, after the application of mathematical models which incorporate the kinetics during adsorption, we and others have shown that thermodynamic and kinetic data, obtained from bath experiments, can be used to predict the position and the shape of the breakthrough curve[2–6].

The comparison of thermodynamic data derived from static bath and dynamic chromatographic experiments was thus of major interest in this investigation. Chromatographic data were obtained by the application of frontal analysis, a technique which lends itself to systematic acquisition of data over a very wide range of experimental and loading conditions. Furthermore, as has been discussed extensively by Jacobsen *et al.*[7] and Kasai *et al.*[8], frontal analysis is an accurate method for quantitative description of the characteristics of the chromatographic adsorption of solutes, including proteins.

In this study, we extend our earlier investigations with a variety of affinity sorbents in the bath experiments to include the use of small-particle-size and non-porous silica-based sorbents (particle diameter, $d_p \leqslant 5$ μm). We were interested to examine whether these sorbents displayed enhanced adsorption performances when used at the upper part of the equilibrium isotherm, or whether they would display the same characteristics shown by large-particle-size sorbents, when used in the overload mode, as reported for zonal chromatographic systems[9].

THEORY

According to Graves and Wu[10], equilibrium isotherms can be measured by static (bath) methods, where discrete points on the isotherms are calculated on the basis of

the concentrations of the adsorbate in solution and the adsorbate in the sorbent. In order to follow the kinetics of adsorption in bath systems, protein concentrations must be monitored continuously by techniques similar to those described by Horstmann *et al.*[11] or by Anspach *et al.*[2]. The results of our previous and current studies clearly demonstrated that bath adsorption methods can display the characteristics of column affinity systems in a realistic way, allowing information about diffusion restrictions of the affinity sorbents to be enunciated. However, there are drawbacks with bath techniques, such as limitations of the type of stationary phases which can be subjected to investigation. Similar conclusions have been reached by Jacobsen *et al.*[7]. Furthermore, when soft gel sorbents are examined in column systems, the structure of the porous network may change as a consequence of the pressure on the bed leading to bed compression. This will influence the permeability and porosity of the gel and at the same time will affect the accessibility of the adsorbate to the immobilized ligands. When thermodynamic and kinetic parameters from bath experiments are employed to design fixed bed procedures, any change in these sorbent characteristics will lead to a significant decrease in separation efficiency, productivity and loadability.

The determination of thermodynamic parameters by means of zonal or frontal chromatographic methods has been described in numerous publications (for reviews see refs. 12–14). As discussed by Jacobsen *et al.*[7] frontal analysis appears to be the method of choice when proteins with relatively large diffusion restrictions are subjected to chromatographic separation. In particular, frontal analysis is particularly suited for adsorbate–ligand interactions when the dissociation constant, K_d, is in the range 10^{-4}–10^{-7} M, *e.g.* ion-exchange, hydrophobic interaction or reversed-phase, metal chelate and some forms of biomimetic and biospecific affinity chromatography. In frontal analysis ideally, after a step increase of the protein concentration at the column inlet, an equivalent step increase in protein concentration should develop at the column outlet when saturation of the column is achieved. Due to mass-transfer resistances (associated with film, pore and surface diffusion and surface reaction resistances) and dispersion effects (mediated by axial, molecular and Eddy diffusion and external dead-volume), the breakthrough front is established as a sigmoidal profile. When the system reaches equilibrium (column inlet concentration equals column outlet concentration), the breakthrough volume can be calculated. This volume at a particular protein concentration corresponds to one point on the equilibrium isotherm. As outlined in our previous publication[2], the feed concentration, c, and solid-phase concentration, q, can be transformed, as required, to yield K_d, the accessible ligand concentration, and the effective capacity of the sorbent, q_m. Using Scatchard plot analysis, the heterogeneity of the affinity sorbents can additionally be recognised.

Using the approach developed by Nichol *et al.*[15], which assumes a Langmuir-type isotherm, the equilibrium constant, K_a, and q_m can be determined without consideration of the shape of the equilibrium isotherm. In the absence of any competing ligand, the relationship between c and q_m can be simplified to

$$\frac{1}{V_e - V_0} = \frac{1}{V_0\, q_m\, K_a} + \frac{c}{V_0\, q_m} \tag{1}$$

where V_e is the breakthrough volume, V_0 the elution volume of a non-retained

component with a molecular weight similar to that of the protein of interest, c is the concentration of the applied feed solution, and q_m is the capacity of the affinity sorbent. For the purposes of the present studies, experimental data were fitted to eqn. 1 by standard methods of numerical analysis.

EXPERIMENTAL

Chromatographic supports

The soft-gel chromatographic support Trisacryl GF 2000 was obtained from Reactifs IBF (Villeneuve la Garenne, France), Cellufine GC 700 Medium from Amicon (Danvers, MA, U.S.A.) and Sepharose CL6B and Blue Sepharose CL6B from Pharmacia LKB (Uppsala, Sweden).

The porous silica-based supports, Spherosil (Type: XOB030) were obtained from Rhône-Poulenc (Usine de Salindres, France); Nucleosil 300-2540, 4000-2540, 300-5, 1000-5, 4000-5 and Polygosil 300-2540 from Machery-Nagel (Düren, F.R.G.). Non-porous silica with a particle size of 1.5 μm was made in our laboratories and is commercially available from E. Merck (Darmstadt, F.R.G.), under the tradename Monospher. Non-porous glass beads were a gift from Polters-Ballotini (Kirchheimbolanden, F.R.G.) and were size-fractionated as described in our previous publication[2].

Chemicals

3-Mercaptopropyltrimethoxysilane (MPS) was obtained from EGA (Steinheim, F.R.G.). Tris, hen egg white lysozyme (E.C. 3.2.1.17, dialysed and lyophilized) and alcohol dehydrogenase (ADH) (E.C. 1.1.1.1, crystallised and lyophilized) from baker's yeast were purchased from Sigma (Sydney, Australia). Cibacron Blue F3GA was obtained from Serva (Heidelberg, F.R.G.). Human serum albumin (HSA) (chromatographically isolated, containing 250 mg/ml protein, 85–130 m*M* sodium chloride and 40 m*M* sodium octanoate) was a gift from the Commonwealth Serum Laboratories (Melbourne, Australia).

Preparation of affinity sorbents

Spherosil XOB030 and Nucleosil 300 were chemically modified with MPS as described in an earlier publication[16]. With silicas of larger pore sizes, such as Nucleosil 1000 and 4000, preliminary investigations established that 5 times the amount of MPS was needed compared to that calculated on the basis of specific surface area and hydroxyl group content. When lower quantities were employed the coverage with MPS was insufficient, and this resulted in low immobilization levels of reactive dyes and non-specific interactions of adsorbed proteins with free hydroxyl groups at the silica surface. Due to the higher silane concentration, the reaction time was reduced to 2 h, in order to avoid polymerization of the silane at the surface of the supports.

The immobilization of Cibacron Blue F3GA on MPS-activated silica and glass beads, and on soft-gel supports was performed as described in refs. 2 and 17.

Chromatographic setup for the frontal analysis experiments

Frontal analysis experiments on soft affinity sorbents and on silica-based and non-porous glass affinity sorbents were performed using the Pharmacia LCC-500

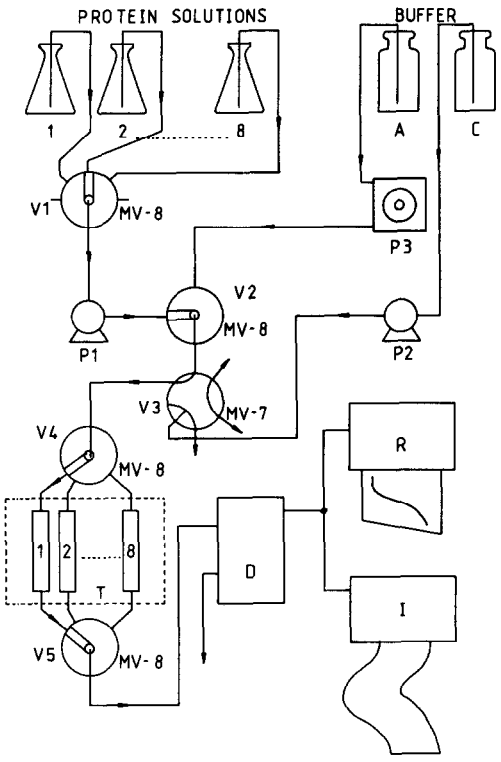

Fig. 1. Schematic diagram of the equipment design used for frontal analysis. Up to eight columns and eight protein concentrations can be investigated with a Pharmacia Fast Protein Liquid Chromatograph in this configuration, with the unit automatically performing under the control of the Pharmacia LCC-500. A: Regeneration buffer [50 m*M* Tris–HCl (pH 7.8) + 2.5 *M* KSCN]; C: equilibration buffer [50 m*M* Tris–HCl (pH 7.8)]; P1: pump for different protein concentrations; P2: pump for equilibration buffer; P3: pump for regeneration buffer; V1: valve for selection of different protein concentrations (eight inlets); V2: valve for the selection of either adsorbate or equilibration buffer; V3: valve for control of either equilibration, adsorption, or wash cycles; V4 and V5: valves for selection of up to eight different columns; D: detector (cell volume: 10 μl, absorbance 280 nm); R: chart recorder; I: integrator (Shimadzu C-R3A); T: thermostat (*e.g.*, at 35.5°C). MV-8 and MV-7 are eight- and seven-port valves, respectively.

system, connected with 4 MV-8 and 1 MV-7 motor valves as outlined in Fig. 1. This chromatographic system was controlled exclusively by the LCC-500. In a single frontal analysis experiment four columns could be tested automatically in a period of 24–48 h, depending on the adsorption capacity of the affinity sorbents. Eight protein solutions of increasing concentrations were applied in each set of experiments, in order to obtain, where possible, data encompassing every part of the isotherm. The dimensions of the affinity columns were 25–35 mm × 5 mm I.D., depending on the adsorption capacity of the affinity gel. Columns were packed by attaching a syringe to one end of each column and applying suction to transfer suspended affinity sorbent to the columns. In order to saturate the active sites on "virgin" chromatographic supports, which lead to non-specific and often irreversible interactions with adsorbed proteins, a solution of 0.2 mg/ml lysozyme was pumped through the columns prior to their experimental use. The columns were then placed in a water bath thermostated at

35.5°C and equilibrated with the regeneration buffer. It should be noted that although this procedure can be used in a practical context to mimic the well documented differences between new and regenerated sorbents, it is appreciated that presaturation of non-specific sites on a sorbent with a particular protein will mask contribution of these sites to the overall adsorption process and could even induce specific protein–protein interactions. Each experimental run was terminated when the test protein concentration at the column outlet was equal to the inlet concentration. The column was regenerated immediately after saturation until no further change in the UV absorption of the effluent was measurable. The regeneration buffer was then maintained in the column, and the next column was investigated via the multiway valves. Each column was equilibrated with the equilibration buffer prior to the adsorption studies with the proteins. After examination of the breakthrough volume of the columns, the valve controlling the protein concentration steps was switched to the next position until the highest concentration was accomplished. The UV absorption at the column outlet was digitalized by an integrator and the equilibrium capacity (q^*) of a given adsorbate concentration (c^*) was evaluated by numerical integration of the area beneath the breakthrough curve. V_e refers to that point of the breakthrough curve where 50% of the amount of adsorbate, as determined by the values of the initial and final condition of the breakthrough curve, was found in the effluent stream. Utilizing this procedure, breakthrough volumes and hence breakthrough times could also be calculated when the corresponding breakthrough curves were not symmetrical around the inflection point. V_0 was determined as the retention volume of a non-retained contaminant of the protein applied to the column.

Evaluation of thermodynamic data

The equilibrium capacity, q^*, was plotted against the corresponding protein concentration, c^*, at the column inlet (see Fig. 2a and b). As described in a prior publication[2], the shape of the isotherm can be utilized to evaluate the type of interaction. q_m and K_d were determined from a double reciprocal plot. In addition, the determination of K_a and of q_m was performed by the method of Nichol *et al.*[15], utilizing eqn. 1.

RESULTS

Comparison of thermodynamic data

Adsorption behaviour of lysozyme. Compared to the values obtained from the corresponding bath experiments[2], affinity constants for lysozyme binding to Cibacron Blue F3GA were considerably lower than affinity constants for HSA, based on the same affinity sorbents and buffer conditions (see Table I). Because of the attenuated interaction of lysozyme with the Cibacron Blue F3GA sorbents in the absence of NaCl, most experiments with this protein were accomplished with at least 0.5 *M* NaCl added to the equilibration buffer. As a result, K_d values for the lysozyme Cibacron Blue F3GA interaction obtained in the presence of 0.5 *M* NaCl were at least one order of magnitude larger than in absence of salt, a result which conforms to K_d values determined with the bath experiments. The interaction of HSA with immobilised Cibacron Blue also decreased in the presence of 0.5 *M* NaCl, but the change in K_d values was far less significant than K_d values derived from the corresponding bath experiments.

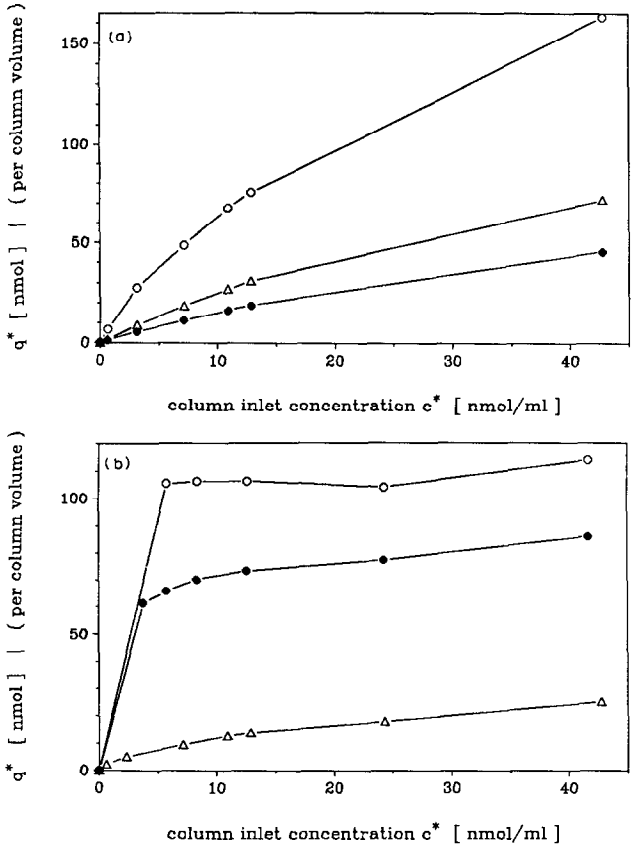

Fig. 2. Equilibrium isotherms for the adsorption of lysozyme on Cibacron Blue F3GA. (a) Adsorption of the protein on the soft-gel sorbents gives typical Langmuir-type isotherms. ○ = Cellufine GC 700; △ = Sepharose CL6B; ● = Trisacryl GF 2000. (b) Adsorption on silica-based affinity sorbents gives rectangular-shaped isotherms for some of the sorbents due to non-specific interactions with the silica surface. ○ = Nucleosil 1000-5; ● = Nucleosil 4000-5; △ = non-porous glass beads (20–40 μm).

The interaction behaviour of lysozyme with the dye affinity sorbents increased on Sepharose and Cellufine chromatographic sorbents with increasing protein concentration, resulting in non-linear Scatchard plots, as evident from Fig. 3. This behaviour was not displayed with the corresponding Trisacryl-based affinity sorbents. The participation of multimodal interactions, including "non-specific" binding effects between lysozyme and other (non-triazine dye) chemical groups accessible on the chromatographic supports as well as protein–protein interactions, must thus be taken into account. This "non-specific" binding behaviour may have its origin in processes that are mechanistically similar to those observed for the interaction between lysozyme and Sephadex G-100 sorbents[15]. When calculation of the thermodynamic parameters was accomplished from data obtained at low and high protein concentrations, affinity constants corresponding to a low and a high affinity binding site could be distinguished, as displayed in Table I. Furthermore, evaluation of the Scatchard plots in terms of a two-component binding model permitted the number of binding sites per

TABLE I

THERMODYNAMIC CONSTANTS FROM FRONTAL ANALYSIS

	q_m (mol/ml)	K_d (M)
Trisacryl GF 2000		
Lysozyme[a]	$2.0 \cdot 10^{-7}$	$4.9 \cdot 10^{-5}$
HSA (without salt)	$9.7 \cdot 10^{-8}$	$5.5 \cdot 10^{-7}$
HSA (with 0.5 *M* NaCl)	$6.1 \cdot 10^{-8}$	$5.7 \cdot 10^{-7}$
Cellufine GC 700		
Lysozyme (low affinity)[a]	$4.0 \cdot 10^{-7}$	$3.6 \cdot 10^{-5}$
Lysozyme (high affinity)[a]	$1.6 \cdot 10^{-7}$	$1.0 \cdot 10^{-5}$
Sepharose CL6B		
Lysozyme (low affinity)[a]	$1.4 \cdot 10^{-7}$	$6.4 \cdot 10^{-5}$
Lysozyme (high affinity)[a]	$7.0 \cdot 10^{-8}$	$2.7 \cdot 10^{-5}$
HSA (without salt)[c]	$2.4 \cdot 10^{-7}$	$6.5 \cdot 10^{-7}$
HSA (with 0.5 *M* NaCl)	$5.1 \cdot 10^{-8}$	$1.5 \cdot 10^{-6}$
Nucleosil 300-2540		
Lysozyme (A)[b] (0.5 *M*)	$1.1 \cdot 10^{-6}$	$4.7 \cdot 10^{-7}$
(B)[b] (0.8 *M*)	$1.5 \cdot 10^{-6}$	$5.4 \cdot 10^{-6}$
Polygosil 300-2540		
Lysozyme (B)[b] (0.8 *M*)	$4.8 \cdot 10^{-7}$	$4.7 \cdot 10^{-7}$
Nucleosil 4000-2540		
Lysozyme (A)[b] (0.5 *M*)	$8.5 \cdot 10^{-8}$	$1.5 \cdot 10^{-6}$
(B)[b] (0.5 *M*)	$2.5 \cdot 10^{-7}$	$1.1 \cdot 10^{-5}$
(B)[b] (0.8 *M*)	$2.2 \cdot 10^{-7}$	$1.2 \cdot 10^{-5}$
(B)[b] (1.2 *M*)	$2.1 \cdot 10^{-7}$	$1.7 \cdot 10^{-5}$
Nucleosil 300-5		
Lysozyme (C)[b] (1.0 *M*)	$9.1 \cdot 10^{-7}$	$2.4 \cdot 10^{-5}$
(B)[b] (0.8 *M*)	$9.0 \cdot 10^{-7}$	$5.5 \cdot 10^{-7}$
Nucleosil 1000-5		
Lysozyme (A)[b] (0.5 *M*)	$3.1 \cdot 10^{-7}$	$3.3 \cdot 10^{-7}$
(B)[b] (0.5 *M*)	$2.5 \cdot 10^{-7}$	$8.3 \cdot 10^{-6}$
(B)[b] (0.8 *M*)	$2.4 \cdot 10^{-7}$	$1.0 \cdot 10^{-5}$
(B)[b] (1.2 *M*)	$2.2 \cdot 10^{-7}$	$1.6 \cdot 10^{-5}$
Nucleosil 4000-5		
Lysozyme (A)[b] (0.5 *M*)	$2.2 \cdot 10^{-7}$	$2.2 \cdot 10^{-6}$
(B)[b] (0.5 *M*)	$1.7 \cdot 10^{-7}$	$1.6 \cdot 10^{-5}$
(B)[b] (0.8 *M*)	$1.7 \cdot 10^{-7}$	$1.8 \cdot 10^{-5}$
(B)[b] (1.2 *M*)	$1.5 \cdot 10^{-7}$	$2.4 \cdot 10^{-5}$
Glass beads fraction 2		
Lysozyme	$3.3 \cdot 10^{-8}$	$< 10^{-5}$
Glass beads fraction 3		
Lysozyme	$1.1 \cdot 10^{-8}$	$< 10^{-5}$
Glass beads fraction 4		
Lysozyme (low affinity)	$4.4 \cdot 10^{-9}$	$2.8 \cdot 10^{-5}$
Lysozyme (high affinity)	$3.8 \cdot 10^{-9}$	$2.3 \cdot 10^{-6}$
Non-porous silica, 1.5 μm		
Lysozyme (C)[b]	$3.3 \cdot 10^{-7}$	$1.3 \cdot 10^{-6}$

[a] Adsorption of lysozyme on Cibacron Blue F3GA-immobilized soft-gel supports was always accomplished with 0.5 *M* NaCl in the adsorption buffer.

[b] Experiments with sorbents prepared from different MPS derivatisation reactions. The dye sorbents derived from these different batches are indicated with (A), (B), and (C).

[c] These data are results from previous investigations[2].

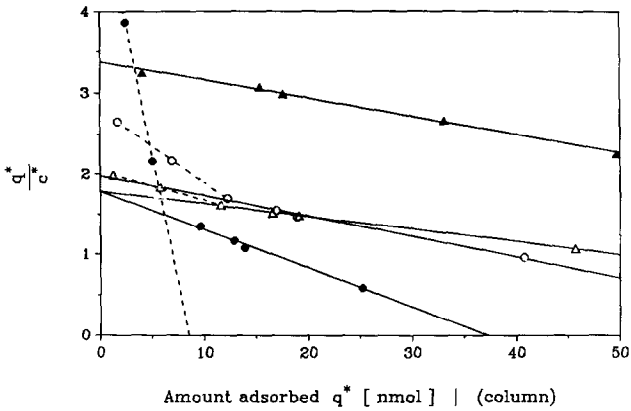

Fig. 3. Scatchard plot analysis of the adsorption of lysozyme on Cibacron Blue F3GA, immobilized on different chromatographic supports. Changes in the mechanism of the affinity interaction can be perceived by changes of the slope of the corresponding graph. (▲) Trisacryl GF 2000: specific adsorption of lysozyme on immobilized Cibacron Blue F3GA only. (△) Sepharose CL6B: at higher lysozyme concentrations protein interactions with low-affinity sites (Sepharose support) cause alteration in the slope of the graph. (○) Cellufine GC 700: deviation from affinity interaction is higher than for Sepharose CL6B. (●) Non-porous glass beads: interaction of lysozyme with the silica surface overrides affinity interaction at low protein concentration.

unit column (or area) of gel matrix to be determined. When determined in this way, the ligand densities associated with the high-affinity sites were (i) generally of lower value compared to those of the "non-specific" low-affinity sites, and (ii) of similar in magnitude to those calculated from the amount of triazine dye immobilised per ml of gel. Consequently, the high-affinity sites were attributed to the immobilized triazine dye ligand, whereas the low-affinity sites were attributed to binding sites on the chromatographic support itself. However, the values of the dissociation constants, associated with these non-specific interactions, were in the same range as those found for the interaction of the protein with the immobilized ligand.

In the column mode, Cibacron Blue F3GA immobilized on Fractogel HW 55, HW 65 and HW 75 sorbents exhibited very little binding with lysozyme and no binding with HSA. Furthermore, leakage of the triazine dyes was observed for all Fractogel sorbents during each chromatographic run. In contrast, when bath experiments were utilized with the same batch of dye immobilised Fractogel affinity gel only small amounts of triazine dye were released during the adsorption experiments. The origin of this anomalous leakage behaviour remains to be determined.

In the matrix systems we have examined, silica-based affinity sorbents prepared under different chemical derivatization conditions occasionally displayed higher affinity constants with lysozyme than the soft-gel sorbents, presumably due to non-specific polar interactions between hydroxyl groups at the silica surface and the basic protein. Associated studies revealed that these free hydroxyl groups were present largely as a result of unsatisfactory modification conditions. When the modification conditions described in the Experimental section were used, these ionic interactions could be minimized and dissociation constants for lysozyme binding to silica-based triazine dye affinity sorbents were in the same range as those obtained for soft-gel affinity sorbents. Furthermore, when adsorption studies were carried out over a range

of salt concentrations (0.8–1.2 *M* NaCl) during the frontal analysis experiments, the derived values of q_m and K_d were also similar (Table I). Association constants for the interaction of the protein with the silica-based sorbents decreased dramatically up to 0.5 *M* NaCl when this salt was added to the buffer, but subsequently did not change substantially in value when higher salt concentrations were utilized (*cf.* Table I). This salt-dependent effect was also reflected in changes in the capacity of the sorbents. These results indicate that for silica-based sorbents the interaction of Cibacron Blue F3GA with lysozyme is protein-specific in the presence of 0.5–1.2 *M* NaCl. When low protein concentrations were utilized, as for the studies with non-porous glass affinity sorbents (size fraction 4), both ionic and biomimetic affinity interactions could be distinguished by Scatchard analysis (Fig. 3). In these cases, the dissociation constant, which corresponded to the low-affinity sites, was found to be comparable to dissociation constants of the soft-gel affinity sorbents associated with specific protein dye interactions.

Based on data provided by the manufacturer on the physical properties of the porous silica supports, the theoretical capacity of silica affinity sorbents was estimated from the known molecular dimensions of the adsorbates. Analogously, the theoretical capacity of non-porous supports was estimated based on their geometric particle dimensions. As anticipated, the effective capacity was less than the theoretical capacity, because portion of the surface area was not accessible to proteins due to steric restrictions. When the estimated and measured capacities of the silica-based dye affinity sorbents were compared, the large-pore-size and non-porous silica sorbents tended to have improved accessibility for the adsorbate, as is evident from Table II. However, our experience with silica-based sorbents over several years has shown that batch-to-batch fluctuations of affinity sorbents from individual reactions with MPS can be significant and result in different capacities and dissociation constants for nominally the same affinity sorbent. The relatively low dissociation constant of the Nucleosil 300 sorbents —compared to the other silica-based sorbents— may be one reason why the capacity of these sorbents is higher. In addition, with non-porous glass beads (or other silicas), polymerization of the silane at the surface of the beads can lead to higher capacities than is theoretically possible on the basis of the geometric dimensions of the particle covered with a monolayer of MPS groups.

As is evident from the data used in Fig. 2a and b, the dissociation constant also influenced the shape of the equilibrium isotherms. For example, when the Cibacron Blue F3GA affinity sorbents were saturated with lysozyme by using very low lysozyme concentration in the feed stock, relatively low values of the dissociation constants and rectangular-shaped equilibrium isotherms were observed. Such isotherms have been previously described by Horváth and co-workers[7,18] and by Kopaciewicz *et al.*[19] for protein ligand binding on ion exchangers and have been attributed to very strong ionic interactions. The determination of thermodynamic constants from rectangular isotherms presents difficulties, because very low protein concentrations must be utilized to obtain data in the ascending part of the isotherm. At such concentrations (*e.g.* below 10 μg/ml), breakthrough times become unacceptably long (in some experiments >24 h with 0.002 mg/ml protein solution) and, in addition, detector or baseline fluctuations can lead to significant errors in the numerically derived values of q_m and K_d. With protein concentrations between 0.01 and 1 mg/ml the evaluation of the dissociation constants from rectangular isotherms is again difficult because the

TABLE II

COMPARISON OF CALCULATED AND EXPERIMENTAL CAPACITIES OF THE SORBENTS

	Experimental capacity (mol/ml)	*Calculated capacity (mol/ml)*	*Ratio of coverage (%)*
Nucleosil 300-2540 (A)[a]	$1.1 \cdot 10^{-6}$	$1.0 \cdot 10^{-5}$	11
(B)[a]	$1.5 \cdot 10^{-6}$	$1.0 \cdot 10^{-5}$	14
Polygosil 300-2540	$4.8 \cdot 10^{-7}$	$1.0 \cdot 10^{-5}$	5
Nucleosil 300-5 (A)[a]	$4.8 \cdot 10^{-7}$	$1.0 \cdot 10^{-5}$	5
(B)[a]	$9.0 \cdot 10^{-7}$	$1.0 \cdot 10^{-5}$	9
Nucleosil 1000-5	$3.1 \cdot 10^{-7}$	$3.1 \cdot 10^{-6}$	10
Nucleosil 4000-5	$2.2 \cdot 10^{-7}$	$1.0 \cdot 10^{-6}$	21
Nucleosil 4000-2540	$8.5 \cdot 10^{-8}$	$1.0 \cdot 10^{-6}$	8
Glass beads (20–40 μm)	$5.5 \cdot 10^{-8}$	$1.1 \cdot 10^{-7}$	52
Glass beads (10–25 μm)	$1.8 \cdot 10^{-8}$	$1.8 \cdot 10^{-7}$	10
Glass beads (5–10 μm)	$3.3 \cdot 10^{-8}$	$4.2 \cdot 10^{-7}$	8
Non-porous silica (1.5 μm)	$3.3 \cdot 10^{-7}$	$2.1 \cdot 10^{-6}$	16

[a] Experiments with sorbents prepared from different MPS derivatisation reactions. The dye affinity sorbents prepared from these batches are indicated by (A) and (B).

sorbents under these conditions may be nearly (or completely) saturated. In addition, small errors in the determination of the protein concentration or breakthrough volume will lead to significant fluctuations in the adsorption capacity. Such errors can result in the calculation of apparent negative dissociation constants, as was observed, for example, in our investigations with lysozyme adsorption on several dye affinity sorbents under low salt-binding conditions. Adsorption of lysozyme on Cibacron Blue F3GA, immobilized on soft-gel supports resulted in an adsorption behaviour reminiscent of Langmuir-type isotherms, as shown in Fig. 2b.

Calculation of thermodynamic constants from breakthrough curves, based solely on application of eqn. 1, will not provide information about the shape of the isotherm. As demonstrated in Fig. 4 for the adsorption of lysozyme on silica-based dye affinity sorbents, in each case with three different sorbents, linear dependencies between $(V_e - V_0)^{-1}$ and column inlet concentration, c^*, were observed, *i.e.* the adsorption process is apparently characterized by eqn. 1. However, as demonstrated in associated studies, the interaction of lysozyme with the silica surface of Nucleosil 300-2540 and Nucleosil 1000-5 sorbent was initially dominant, due to the high affinity constant for the binding of the silica surface sites with the protein. As a consequence, data on the specific, biomimetic binding of the dye ligand with the protein were only available from the upper part of the equilibrium isotherm. Because of the limitations described above, regression analysis of the frontal analysis data corresponding to the adsorption of lysozyme to Cibacron Blue F3GA, immobilized on Nucleosil 300-2540, resulted in a negative value of the $(V_e - V_0)^{-1}$ intercept at $c^* = 0$. The low dissociation constant corresponding to the specific adsorption with the Nucleosil 1000-5 sorbent is questionable, on the basis of the same argument.

Adsorption behaviour of HSA and ADH. Adsorption of HSA on the Trisacryl GF 2000 and Sepharose CL6B dye affinity sorbent in packed columns displayed almost the same accessible ligand concentrations as were found in the bath

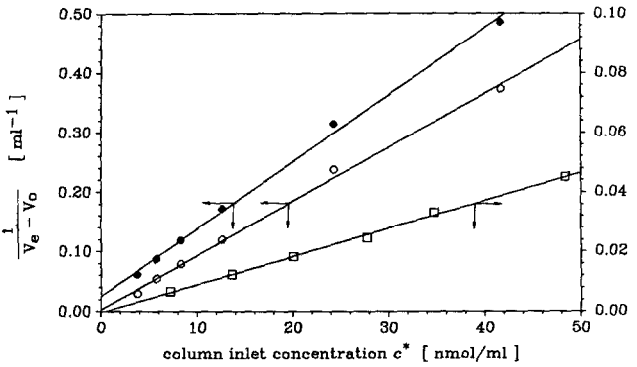

Fig. 4. Evaluation of thermodynamic constants from frontal analysis experiments by application of eqn. 1. □ = Nucleosil 300-2540; ○ = Nucleosil 1000-5; ● = Nucleosil 4000-5.

experiments[2] (*cf.* Table III). The value of the dissociation constants determined by these two methods differred by $<15\%$. This difference may simply reflect the specific experimental conditions, since the average adsorbate concentration range in the frontal analysis experiments was usually higher than in the bath experiments. Furthermore, we experienced more frequent data fluctuation in the equilibrium isotherm data in the column experiments than in the bath experiment. Due to very slow adsorption kinetics during the adsorption of HSA on the Cellufine GC 700 dye sorbent, no thermodynamic constants could be determined with this system. Since HSA could not be desorbed from the silica- and glass-based affinity sorbents, these sorbents were also excluded from frontal analysis experiments.

The adsorption of ADH on Blue Sepharose CL6B appears to be mainly controlled by mass-transfer restrictions, and this results in an early breakthrough of the protein, as shown in Fig. 5. This result was in contrast to the corresponding bath experiments where ADH was adsorbed on Blue Sepharose CL6B at a relatively rapid rate. Since the breakthrough volume, as calculated by numeric integration from the breakthrough curve, did not show a dependency on the increasing protein concentrations, as predicted by eqn. 1, calculation of thermodynamic data was not possible. One

TABLE III

COMPARISON OF THERMODYNAMIC CONSTANTS FROM FRONTAL ANALYSIS AND BATH EXPERIMENTS

	Frontal analysis		*Bath experiment*	
	q_m *(mol/ml)*	K_d *(M)*	q_m *(mol/ml)*	K_d *(M)*
Trisacryl GF 2000				
Lysozyme	$2.0 \cdot 10^{-7}$	$4.9 \cdot 10^{-5}$	$4.7 \cdot 10^{-6}$	$1.2 \cdot 10^{-3}$
HSA (without salt)	$9.7 \cdot 10^{-8}$	$5.5 \cdot 10^{-7}$	$7.8 \cdot 10^{-8}$	$1.0 \cdot 10^{-6}$
HSA (+ 0.5 *M* NaCl)	$6.1 \cdot 10^{-8}$	$5.7 \cdot 10^{-7}$	$6.4 \cdot 10^{-8}$	$2.1 \cdot 10^{-6}$
Sepharose CL6B				
HSA (without salt)	$2.4 \cdot 10^{-7}$	$6.5 \cdot 10^{-7}$	$4.9 \cdot 10^{-8}$	$5.2 \cdot 10^{-7}$
HSA (+ 0.5 *M* NaCl)	$5.1 \cdot 10^{-8}$	$1.5 \cdot 10^{-6}$	$6.8 \cdot 10^{-8}$	$7.3 \cdot 10^{-7}$

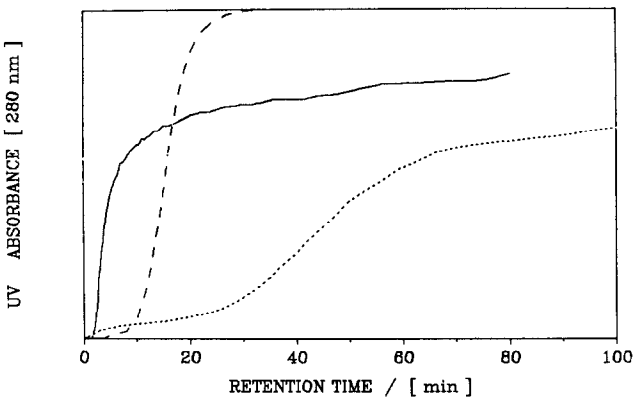

Fig. 5. Shape of the breakthrough curve and retention volumes during the adsorption of proteins on Blue Sepharose CL6B. Flow-rate, 0.3 ml/min. --- = Lysozyme (hen egg white, 0.05 mg/ml); ···· = serum albumin (human, 0.33 mg/ml); ——— = alcohol dehydrogenase (yeast, 0.02 mg/ml).

reason for this early breakthrough of ADH in the frontal analysis experiments with Blue Sepharose CL6B would appear to be a consequence of aggregation of ADH at the selected protein concentrations. The average concentration of the feed solution was higher in the frontal analysis experiments than in the corresponding bath experiments. In addition, deformation of the soft-gel sorbent, which has its origin in the mechanical properties of the gels, led to deformation of pore entrances and/or connectivity of the network of the sorbent. Evidence for the elastic deformation of Sepharose gels occurring during the packing procedure or as a consequence of the pressure associated with the flow-rate is well known. In the present studies, the bed volume decreased approximately 30% over the flow-rate range of 0.3–0.5 ml/min. Both effects result in an increase of diffusion restrictions and, consequently, slower adsorption kinetics.

Evaluation of the experimental data for all three proteins (lysozyme, HSA and ADH) as breakthrough curves obtained with the dye affinity sorbents in terms of the chromatographic model developed by Nichol *et al.*[15] or by double reciprocal plots, derived from equilibrium isotherms, resulted in values of the thermodynamic constants that were in close agreement for all affinity sorbents (*cf.* Table I). Deviations, which were never greater than 10% from predicted values with these different theoretical models, could be attributed to the sample rate of data acquisition by the detector integrator, which varied from 1 datapoint per 15 s to 1 datapoint per 120 s, depending on the capacity of the sorbent and the protein concentration used for the experiment.

Comparison of breakthrough curves

The capacity of affinity sorbents and the dissociation constant of the affinity complex are reflected in the retention volume of the breakthrough curve. Similarly, the kinetics during adsorption of the protein to the dye affinity sorbent are reflected in the shape of the breakthrough curve. As demonstrated in Fig. 6, normalised retention times for lysozyme shifted significantly when dye affinity sorbents with higher binding capacity, such as the Nucleosil 1000-5-derived sorbent, were employed under the same chromatographic conditions. Due to the relatively small capacity of the Sepharose and

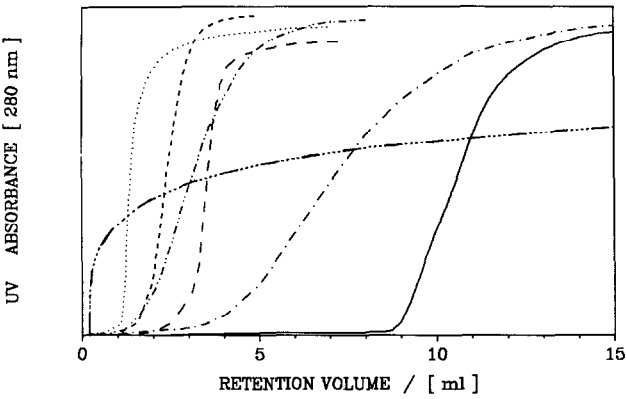

Fig. 6. Shape of the breakthrough curve and retention volume of various chromatographic sorbents with different pore sizes and particle sizes during the adsorption of lysozyme. Flow-rate, 0.5 ml/min; protein concentration, 0.10 mg/ml. ——— = Nucleosil 1000-5 (5 μm); – – – = Nucleosil 4000-2540 (25–40 μm); - - - - - = Sepharose CL6B (40–165 μm); – · – · – = Trisacryl GF 2000 (40–80 μm); – · – · – = Cellufine GC 700 (45–105 μm); – · · · · – · · · · = Spherosil XOB030 (100–300 μm); · · · · · · · · · = non-porous glass beads (20–40 μm).

Trisacryl dye affinity sorbents for lysozyme, the solute breakthrough occurred relatively early in the chromatogram. In contrast, the Cellufine sorbent, which contained a higher Cibacron Blue F3GA density, was capable of adsorbing more lysozyme than the other soft-gel sorbents. However, the pore size of this sorbent is relatively small (pore diameter <40 nm), and this resulted in shallower breakthrough curves. Because of the small pore size of this matrix, the adsorption of HSA on the Cellufine GC 700 dye affinity sorbent was a very slow process, resulting in a shape of the breakthrough curve similar to that displayed in Fig. 6 for the adsorption of lysozyme on the Spherosil XOB030 dye affinity sorbent. These results suggest that the Cellufine GC 700-based affinity sorbent will be unsuitable for the high-capacity adsorption of proteins with molecular weights larger than 20 000.

Although silica gel affinity sorbents displayed lower dissociation constants when only partial modification of the silica surface was accomplished, the steepness of the breakthrough curve was largely dependent on the pore size. Breakthrough curves obtained with low lysozyme concentrations and the Nucleosil 4000 dye affinity sorbents with particle sizes of 5 μm were steeper than the corresponding 25 to 40-μm-diameter sorbents, as illustrated in Fig. 7. At higher protein concentrations, which corresponded to the plateau of the equilibrium isotherm, only minor differences could be observed in the shape of the breakthrough curve for both types of Nucleosil-based sorbents of different particle diameter. This behaviour is similar to that observed in zonal chromatography, where the number of theoretical plates per column volume decreases more dramatically with small particle sizes than with large particles, when the column is operated in the overload mode[9]. In particular, major differences occurred at the onset of the breakthrough curves when small-particle or non-porous dye affinity sorbents were employed, and this resulted in a rapid increase in the protein concentration at the column outlet. As saturation was approached, the shape of the breakthrough curves became similar for sorbents of different particle size.

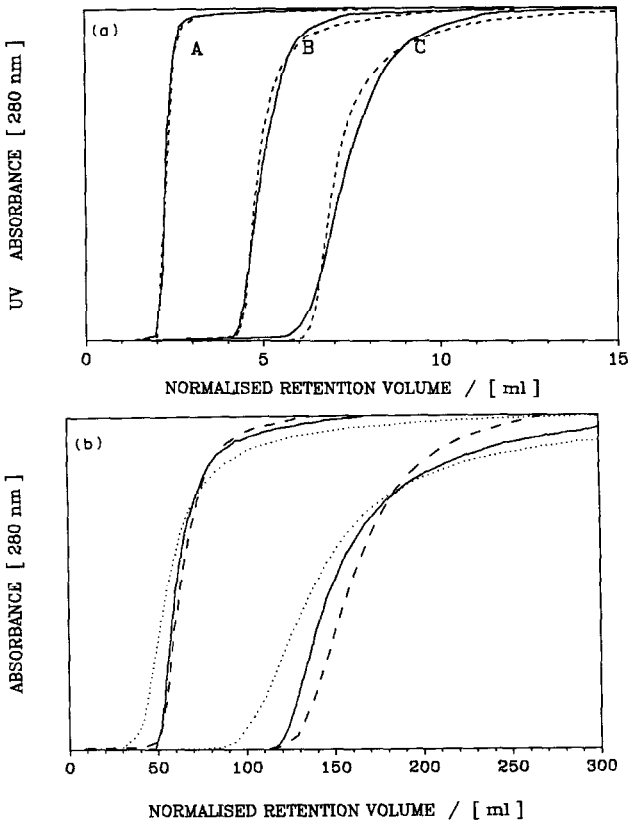

Fig. 7. Profile of breakthrough curves on silica-based affinity sorbents with different particle sizes but constant pore size during the adsorption of lysozyme in 50 m*M* Tris–HCl (pH 7.8)/0.8 *M* NaCl at a flow-rate of 0.5 ml/min. (a) ----- = Nucleosil 4000-5; ——— = Nucleosil 4000-2540; (protein concentration, A = 1.0 mg/ml, B = 0.2 mg/ml, C = 0.05 mg/ml). (b) ····· = Polygosil 300-2540; ----- = Nucleosil 300-2540; ——— = Nucleosil 300-5 (protein concentrations, 1.0 mg/ml and 0.2 mg/ml).

This adsorption behaviour resulted in rather asymmetrical curves when small-particle-size sorbents were utilized. During investigation of breakthrough curves at three different salt concentrations (0.5 *M*, 0.8 *M*, and 1.2 *M* NaCl) but under otherwise identical conditions, the normalised breakthrough curves for the 5-μm particles crossed the breakthrough curves of the 25- to 40-μm particles a second time near the saturation point, indicating that overall adsorption was slower, or at least of similar rate in this region of the breakthrough curve (*cf.* Fig. 7). The most shallow breakthrough curves and therefore the silica-based dye affinity sorbent which performed poorest in our tests, was the Polygosil 300-2540 dye sorbent. This sorbent is based on an irregularly shaped silica with characteristics claimed by the manufacturer to be otherwise indentical with those described for the Nucleosil 300-2540 support.

As noted above, asymmetrical shapes of the breakthrough curves were evident with all small-sized silica affinity sorbents and were extremely marked when non-porous glass beads or silica beads were used (see Fig. 6). This type of breakthrough phenomenon might be based on secondary equilibrium effects,

associated with the rearrangement of already adsorbed proteins. Similar breakthrough shapes have been found for the adsorption of lysozyme on monoclonal antibodies immobilized on non-porous, activated silicas[6] and the adsorption of trypsin on non-porous benzamidine sorbents[16].

DISCUSSION

This study documents the further use of MPS for the chemical modification of microparticulate glasses and silicas. Under reaction conditions where the molar ratio of introduced silane to the silanol group content is maintained constant affinity sorbents with different levels of dye ligands are generated when silica particles of different pore sizes or non-porous glass and silica beads are used. For example, a 5-fold increase in the amount of MPS, based on the theoretical quantity required for the large-pore-size silicas Nucleosil 1000 or 4000 was needed to achieve comparable immobilization levels of Cibacron Blue F3GA to that obtained with small-pore-size silicas Nucleosil 300. A consequence of increasing the MPS concentration in the modification reaction with silicas is however increased polymer coverage by the silane. This has a subsequent effect on the protein adsorption capacity of the dye-affinity sorbent. Typical of these effects are the results obtained with the non-porous glass beads where the polymerization levels increased with increasing particle size, leading to higher immobilization levels of Cibacron Blue F3GA than would be theoretically possible, based on the geometric dimensions of the particle and its known silanol content. Although non-specific protein silanol or protein silane polymer interactions could not be suppressed completely, as demonstrated, *e.g.* in Fig. 3 by the Scatchard plots for non-porous glass affinity sorbents, interactions between the protein and polymerized silane molecules were found to be less important than interactions between the protein and hydroxyl groups at the silica surface. Furthermore, the polymerization of the silane at the silica surface also does not appear to influence the overall adsorption kinetics dramatically, because breakthrough curves for non-porous glass affinity sorbents and also for Nucleosil 4000-5 showed nearly rectangular profiles typical of very good adsorption characteristics. However, the capacities of the non-porous glass dye affinity sorbents were considerably lower than those of the porous silica and soft-gel affinity sorbents.

Dissociation constants for the affinity interactions of lysozyme with Cibacron Blue F3GA, immobilized on soft gel as well as silica sorbents, were generally one order of magnitude higher when 0.5 *M* NaCl was added to the equilibration buffer. This indicates that the adsorption mechanism in the absence of salt might be controlled mainly by ionic interactions of oppositely charged groups on the dye and protein molecules. Results reported by Chase[3] for the adsorption of lysozyme on Blue Sepharose CL6B in the absence of NaCl also demonstrated dissociation constants ($K_d = 1.7 \cdot 10^{-6}$ *M*) that were lower than ours for salt-free silica-based systems. Increasing the concentration of NaCl above 0.5 *M* did not significantly affect the dissociation constant and this suggests that specific biomimetic affinity interactions contribute to the adsorption under these conditions.

As is evident from Fig. 5 for the adsorption of lysozyme to Spherosil XOB030 and from Fig. 6, showing the adsorption of ADH on Blue Sepharose CL6B, breakthrough curves characteristic of unusual adsorption behaviour, typically

associated with the breakthrough of a portion of the selected protein solution at V_0, were observed. This behaviour was also observed for the adsorption of HSA on Cellufine GC 700 dye affinity sorbents and may be related to the split peak phenomenon in zonal chromatography. This phenomenon occurs when sorbents with high mass-transfer restrictions are employed for the separation of proteins under conditions of relatively high flow-rates[20,21]. Under these experimental conditions, two peaks can be observed for a single protein, the relative abundance of the two zones depending on the flow-rate. Using sorbents exhibiting a relatively high ratio (λ) of protein size to pore size, a percentage of the adsorbate will not be able to enter the porous system nor will it be able to interact with the outer surface of the sorbent due to prior saturation of these external binding sites. A portion of the protein concentration will therefore pass through the column without interaction. This behaviour will be particularly important in protein particle system involving (i) long diffusion pathways of the adsorbate from the eluent stream to the outer surface of the sorbent, (ii) significant mass-transfer restrictions at pore entrances and (iii) significant film thickness of stagnant mobile phase surrounding each particle. When unusual shapes of the breakthrough curve were observed for the protein adsorption on the immobilised dye sorbents, these curves were invariably associated with long adsorption times and an almost horizontal progress of the adsorption curve. Due to the small but monotonously incremental changes in adsorption it is difficult to judge when the system had reached equilibrium. Even when this problem is overcome, as was achieved for the adsorption of ADH on Blue Sepharose, the determination of thermodynamic constants for some protein systems still remains problematical. For example, when human immunoglobulin G (IgG) was adsorbed on Cibacron Blue-immobilized Sepharose CL6B, the breakthrough volumes monotonously increased over the protein concentration range from 0.04–0.32 mg/ml. Instead of being anticipated by eqn. 1 for all human IgG concentrations, the calculated breakthrough volumes continued to change with increasing protein concentration when a particular protein concentration was exceeded. Although human IgG has a molecular weight similar to that of ADH, the adsorption of this protein may involve a different interaction mode[22]. The explanation for such specific behaviour may have its origin in the inability of all adsorbate molecules to interact with the dye affinity sorbent due to steric effects, some protein molecules being simply flushed through the column and therefore not being accounted for in the equilibrium equation.

Some dye affinity systems showing typical adsorption behaviour in the bath experiments[2], such as the HSA/Cellufine GC 700 sorbent system or the ADH/Blue Sepharose sorbent system, also displayed very slow adsorption kinetics and early breakthrough of proteins occurred when they were used as packed columns. In case of the Fractogel dye sorbents, no noticeable adsorption occurred of any of the three proteins in the column mode. These unexpected results may have their origin in changes in the gel structure of these sorbents as a result of the operating conditions, such as the influence of flow-rate and attendant pressure on the bed. In the column systems the porous structure of the Fractogel dye sorbents is significantly deformed so that even lysozyme could not penetrate the porous system. These changes observed in the adsorption kinetics with column systems clearly illustrate a major limitation of the bath model. Although the thermodynamic constants from bath and column experiments with several protein dye sorbent systems corresponded very well, where changes

in the gel structure were not dominant or could not occur, for other dye affinity systems the data from the bath experiments did not agree with the column experiments. Consequently, comparative behaviour of the bath and column model can only be expected for sorbents having a rigid gel structure, such as silica-based sorbents, where no significant deformation of the porous network structure occurs. The nature of the dependency of pressure drop, Δp, upon flow-rate for a packed column may thus be an important parameter in comparing bath and column models of adsorption behaviour, *i.e.* whether the dependency is linear over a wide range of flow-rates or exhibits the asymptotic behaviour characteristic of many soft gels at higher flow-rates.

Sorbents based on small-particle-size supports generally showed steeper breakthrough curves and therefore better performance than the large-particle-size sorbents in the lower part of the breakthrough curve. With the non-porous dye sorbents based on either silica or glass beads, a nearly rectangular shape was observed. However, the shape of the breakthrough curve with these high-performance sorbents was never symmetrical around the inflection point and when compared to large-particle-size sorbents the adsorption process displayed considerably slower adsorption kinetics in the upper part of the curve than in the lower part (*cf.* Fig. 7). This adsorption phenomenon was also observed in our previous studies, when non-porous silica supports were employed as sorbents in frontal analysis experiments with immobilized ligands, such as benzamidine for the adsorption of trypsin[16] and with monoclonal antibodies against lysozyme[6]. The relatively slow adsorption kinetics for proteins displayed in the upper part of the breakthrough curves may be attributable to a rearrangement of adsorbed proteins, which in the initial phase of adsorption are statistically distributed at the surface of the sorbent, but become more densely packed towards the end of the adsorption process. In addition, a reorientation of adsorbed proteins may also take place, directed by specific protein–protein and protein–ligand interactions and leading to the most favoured arrangement of adsorbed proteins at the surface of the sorbent. Such a phenomenon would be less apparent when large particle/pore-size sorbents are employed, since in these cases adsorption of proteins is mainly diffusion-controlled throughout the adsorption process and rearrangement of adsorbed proteins might occur with a similar time scale to diffusional transport. To substantiate this hypothesis, more studies are needed at much lower protein concentrations than utilized in the present study in order to provide data relevant to the linear part of the equilibrium isotherm.

Apart from the asymmetric breakthrough curves discussed above, the adsorption kinetics in the upper part of the curve were consistently slower with small-particle-size than with larger-particle-size sorbents at identical protein concentrations. In order to equate adequately the effect of particle size for various sorbent systems, the experimentally determined breakthrough volumes for sorbents with different particle sizes were corrected by appropriate multiplication factor in order to yield normalized values. Reevaluation of the data then revealed an inverse relationship between adsorption kinetics and particle size for protein loads approaching saturation. This dependency may have its origin in one or more of the possibilities discussed below.

Non-ideal pore connectivity

The particle-size/pore-size ratio of Nucleosil 4000-5 is very low (12.5) compared to Nucleosil 4000-2540 (>62.5). Supports having particle-size/pore-size ratios of <30

are, based on the theoretical considerations of Guiochon and Martin[23], presumed to experience unimpeded flow through the porous system. However, Nucleosil supports have been reported[24] to show lower performance in size-exclusion chromatography than expected for their particle size. A similar phenomenon might occur during frontal analysis, since the pathway of the protein through the porous system will be impeded by non-ideal pore connectivity. Since residence times of the protein inside the pores of the sorbent will then be shorter, breakthrough might occur earlier and at lower protein concentrations, whilst protein–ligand rearrangements could become more dominant at higher protein concentrations. Further experiments, in which dye affinity sorbents with pore sizes of 30 nm, 100 nm and 400 nm, and a particle size of 5 μm are compared, may confirm this hypothesis. In this connection it is noteworthy that the data for Nucleosil 1000-5 which has a particle-size to pore-size ratio of 50, demonstrated that this dye affinity sorbent performed best in terms of kinetic phenomena (*cf.* Fig. 8).

Ligand gradients

Ligand heterogeneities (denser immobilized ligands at the surface than at the centre of the sorbent) have been previously discussed as a major factor in adsorption anomalies. The current evidence[24] on this aspect suggests that for small-particle-size sorbents, chemical modification of the matrix surface results in a more homogeneous layer of immobilized ligands over the accessible surface of the particle than for large-particle-size sorbents. Furthermore, more homogeneous sorbents are believed to perform better than heterogeneous sorbents. In this respect the 5-μm sorbents should perform better, than, *e.g.*, a 25-μm porous sorbent. In our studies, this could only be confirmed at the lower part of the breakthrough curve, but never at the upper part. If rearrangement and, possibly, reorientation of adsorbed proteins[25] are a major contributing factor to the adsorption kinetics at the upper part of the breakthrough curve, no real justification exists *a priori* why sorbents with a more homogeneous ligand densities and distribution over the whole surface of the particle should perform better than those with a ligand gradient in the pores. Sorbents having lower ligand

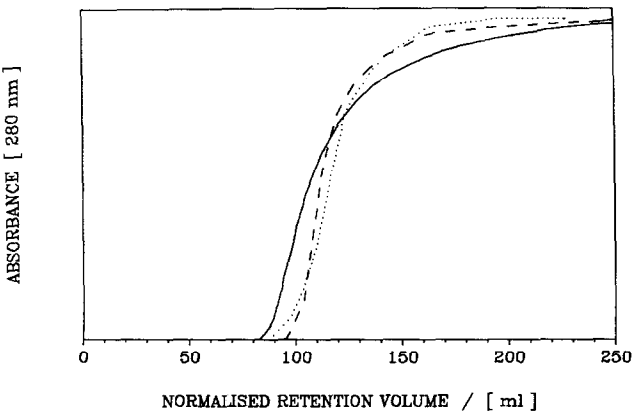

Fig. 8. Profile of breakthrough curves on silica-based affinity sorbents with different pore sizes and constant particle size during the adsorption of lysozyme in 50 m*M* Tris–HCl (pH 7.8)/0.8 *M* NaCl at a flow-rate of 0.5 ml/min. ····· = Nucleosil 300-5; ----- = Nucleosil 1000-5; ——— = Nucleosil 4000-5.

densities in the centre of the sorbent than at the outer surfaces may conceivably display better adsorption characteristics and kinetics due to much more specific interaction of the adsorbate with the ligand, in which case reorientation will not be necessary. Invoking this hypothesis would explain the better performance of large particle-size sorbents of both the Nucleosil 300- and Nucleosil 4000-based supports (*cf.* Fig. 7a and b).

Changes in dissociation constants

Differences in the adsorption capacities and dissociation constants of the various dye affinity sorbents can be considered as an obvious explanation of the observed dependence of kinetics on particle sizes in the overload condition. As shown in Table I, the capacity of the Nucleosil 4000-2540 dye affinity sorbent was higher and the dissociation constant was lower than that of the Nucleosil 4000-5 dye affinity sorbent, whilst for the Nucleosil 300 dye affinity sorbents, the opposite was observed. If the kinetic effect was solely due to differences in the dissociation constants, one would expect the breakthrough curve behaviour of Nucleosil 300 and Nucleosil 4000 to be different. Since this was not the case (*cf.* Fig. 7a and b), other influences, besides dissociation constant differences, must be involved.

CONCLUSIONS

With preparative batch chromatographic isolations, feed stock loading of proteins is interrupted when a certain amount of the protein of interest is detected in the effluent. In such situations, slow adsorption kinetics in the upper part of the breakthrough curve will not represent a serious limitation in terms of productivity or performance. If protein rearrangement and/or reorientation plays a central role in the adsorption, for sorbents containing more immobilized ligands than required on a stoichiometric basis to bind the adsorbate (*i.e.* excess ligands are always available) then, the effective capacity of these "high-ligand-density" sorbents may not necessarily be higher than the capacity of a sorbent with a lower amount of immobilized ligands. In such "high-ligand-density" cases a proportion of the immobilized ligands may not be accessible whilst high density patches of ligands may even contribute to slower adsorption kinetics. The use of small-particle-size sorbents will not circumvent this limitation. Beside the technical and economic issues of pressure, cost of manufacture, and packing requirements, the use of small-particle sorbents (*e.g.*, $d_p < 10$ μm) in preparative chromatography does not appear to be justified, especially, if a breakthrough of 10% or 20% of the protein of interest can be tolerated. Such conditions occur commonly in large-scale chromatographic isolations involving recycling capabilities. Collectively, these conclusions argue in favour of larger-particle-diameter sorbents in process applications.

An important outcome of the studies discussed in this publication is the further demonstration of the usefulness of the chromatographic model, based on frontal analysis, in characterizing and providing essential data on the thermodynamic parameters and the dynamic performance of sorbents. Changes in the adsorption behaviour of proteins due, *e.g.*, to steric hindrances is not as obvious in bath experiments and may not be recognized. Furthermore, the influence of changes in the gel structure after packing the columns, as observed for the Fractogel and Blue

Sepharose sorbents, will also not be recognised, if only bath experiments are considered.

The adsorption of proteins on sorbents is still a poorly understood and obviously a very complex process. Interpretation of observed adsorption phenomena often cannot be adequately explained by first order models, which account only for homogeneous protein–ligand interaction. Irreversible adsorption, as observed for example with HSA and some silica-based affinity sorbents, may ultimately become predictable if a full picture of the molecular basis of protein–protein interactions, protein unfolding, or rearrangement of the tertiary structure and reorientation of proteins at the surface of the sorbent were available. To account for —and predict— such effects, much more information about the molecular events occurring between proteins and their environment in adsorption on biomimetic affinity sorbents remains to be acquired. Approaches to such studies on protein adsorption and chromatographic behaviour form part of associated investigations to be described in subsequent publications[25,26]. As eloquently noted by Jacobsen *et al.* in a seminal publication[7] on the measurement of adsorption isotherms "The continued importance of adsorption and chromatographic processes in various areas of science and technology has made them a common focus of study".

ACKNOWLEDGEMENTS

The support of the Australian Research Grants Committee and Monash University Special Research Grants (to M.T.W.H.) is gratefully acknowledged. F.B.A. is a recipient of a Monash University Postdoctoral Fellowship. Furthermore this work was part of a research project supported by the Deutsche Forschungsgemeinschaft, F.R.G. A.J. is a recipient of a Monash Univerisity Graduate Scholarship.

REFERENCES

1 M. Guthridge, J. Bertolini and M. T. W. Hearn, *J. Chromatogr.*, 476 (1989) 445.
2 F. B. Anspach, A. Johnston, H.-J. Wirth, K. K. Unger and M. T. W. Hearn, *J. Chromatogr.*, 476 (1989) 205.
3 H. A. Chase, *J. Chromatogr.*, 297 (1984) 179.
4 F. H. Arnold, S. A. Schofield and H. W. Blanch, *J. Chromatogr.*, 355 (1986) 1.
5 B. H. Arve and A. T. Liapis, *AIChE J.*, 33 (1987) 179.
6 A. T. Liapis, B. Anspach, M. F. Findley, J. Davies, K. K. Unger and M. T. W. Hearn, *Biotechnol. Bioeng.*, (1989) in press.
7 J. Jacobsen, J. Frenz and Cs. Horváth, *J. Chromatogr.*, 316 (1984) 53.
8 K.-I. Kasai, Y. Oda, M. Nishikata and S.-I. Ishi, *J. Chromatogr.*, 376 (1986) 33.
9 G. Guiochon and A. Katti, *Chromatographia*, 24 (1987) 165.
10 D. J. Graves and Y.-T. Wu, *Methods Enzymol.*, 34 (1974) 140.
11 B. J. Horstmann, C. N. Kenney and H. A. Chase, *J. Chromatogr.*, 376 (1986) 179.
12 I. M. Chaiken, *J. Chromatogr.*, 376 (1986) 11.
13 D. J. Winzor and E. J. Yon, *Biochem. J.*, 217 (1984) 867.
14 F. H. Arnold, H. W. Blanch and C. R. Wilke, *Chem. Eng. J. (Lausanne)*, 30 (1985) 9.
15 L. W. Nichol, A. G. Ogston, D. J. Winzor and W. H. Sawyer, *Biochem. J.*, 143 (1974) 435.
16 B. Anspach, H. J. Wirth, K. K. Unger, P. Stanton, J. Davies and M. T. W. Hearn, *Anal. Biochem.*, 179 (1989) 171.
17 B. Anspach, K. K. Unger, J. Davies and M. T. W. Hearn, *J. Chromatogr.*, 457 (1988) 195.
18 A. Yelayudhan and C. Horváth, *J. Chromatogr.*, 443 (1988) 13.
19 W. Kopaciewicz, S. Fulton and S. Y. Lee, *J. Chromatogr.*, 409 (1987) 111.

20 L. A. Larew and R. R. Walters, *Anal. Biochem.*, 164 (1987) 537.
21 C. DeLisi, H. W. Hethcote and J. W. Brettler, *J. Chromatogr.*, 240 (1982) 283.
22 P. G. H. Byfield, S. Copping and R. L. Himsworth, *Mol. Immunol.*, 21 (1984) 647.
23 G. Guiochon and M. Martin, *J. Chromatogr.*, 326 (1985) 3.
24 K. K. Unger, *Porous Silica*, Elsevier, Amsterdam, 1984.
25 M. T. W. Hearn, M. I. Aguilar and A. N. Hodder, *J. Chromatogr.*, in press.
26 M. T. W. Hearn, A. N. Hodder and M. I. Aguilar, submitted for publication.